

## ULTRA WIDE BAND RESPONSE OF AN ELECTROMAGNETIC WAVE SHIELD BASED ON A DIODE GRID

Yangjun Zhang<sup>1, \*</sup>, Mengqing Yuan<sup>2</sup>, and Qing Huo Liu<sup>3</sup>

<sup>1</sup>Department of Electronics and Informatics, Ryukoku University, Seta, Ohtsu 520-2194, Japan

<sup>2</sup>Wave Computation Technologies, Inc., Durham, NC 27707, USA

<sup>3</sup>Department of Electrical and Computer Engineering, Duke University, Durham, NC 27708-0291, USA

**Abstract**—This paper investigates Ultra Wide Band (UWB) response of a self-actuated electromagnetic wave shield based on a diode grid both in frequency and time domain. The investigation is first carried out on a shield valid for an incident wave polarized at a specific direction only, then extended to a shield effective for an incident wave polarized at an arbitrary direction. In the frequency domain, two linear analysis methods are used to study the properties of the diode grid over the frequency range from 0.01 to 10 GHz. One method is the microwave network analysis. Another is simulating the diode grid by a linear equivalent circuit instead of a diode. In the time domain, the property of the shield is studied with respect to a broadband impulse, where the diode is described by its SPICE circuit model including the nonlinear property. The results show that the diode grid works well as a self-actuated electromagnetic power selective surface (PSS) in a certain frequency range. The diode grid is strongly frequency dependent. The operating frequency band relies on the reactive elements in the diode grid. In order to extend the operating frequency to a high band, smaller cell size and smaller junction capacitance should be employed.

---

*Received 30 May 2013, Accepted 20 July 2013, Scheduled 5 August 2013*

\* Corresponding author: Yangjun Zhang (zhang@rins.ryukoku.ac.jp).

## 1. INTRODUCTION

RF and microwave assets such as antennas, radars and lens systems, and their associated circuitries are necessary to be protected from strong incident electromagnetic waves which are intentionally or unintentionally introduced. Meanwhile, the systems are required to operate well in the designed electromagnetic environment. Radome shutter is usually used for antenna or radar system protection. It cuts off all incoming electromagnetic waves when the equipment is not operating, and permits the waves in the desired frequency range to be transparent during operation. A wire mesh or conductive coating is another simple and effective shield for unwanted frequency components. Its transmission and reflection properties have been reported in [1,2]. However, both wire mesh and radome have a significant disadvantage. The principle of a radome or frequency selective surface (FSS, such as a wire mesh) shows that the intentional strong electromagnetic energy is still possible to damage the equipment within the operating frequency band.

Self-actuated protection is considered as a good solution to protect such RF and microwave assets from strong electromagnetic interference. It is transparent to the protected system at certain signal level, but shows protection from strong electromagnetic interference. Plasma limiter is one kind of equipment for self-actuated protection [3–5]. Gas will be ionized by a high microwave power, and then reflect the incident energy. Self-actuated protection can also be realized by a power selective surface (PSS), which is constructed by field-induced conductivity material whose surface impedance depends on the intensity of electromagnetic field [6, 7].

Recently, a high frequency diode grid was proposed for self-actuated protection. Different from the active diodes used in FSS reported early [8–10], the diodes in self-actuated protection are directly triggered by the impinging electromagnetic wave. Thus, a bias network is not required. The examples are the limiting frequency selective surface in [11], and the diode grid in [12]. The diode or diode grid are shown self-actuated protection in these reports. However, the investigated frequency band in these studies is narrow. For example, the limiting FSS controlled by the diodes is designed to operate from 2.0 to 4.0 GHz [11]. The experiment on diode grid is only carried out around 1.0 GHz [12]. Therefore, the performance of this FSS at other frequencies is still unknown. It is necessary to study the property of the diode grid over a wide frequency band.

This paper investigates the UWB response of an electromagnetic wave shield based on a diode grid by theoretical analysis and by

a commercial full wave transient field simulator integrated with the nonlinear SPICE circuit solver [13]. In Section 2, the structure and basic principle of an electromagnetic wave shield based on a diode grid are shown. In Section 3, we use two linear analysis methods to study UWB response of the diode grid in the frequency domain. One method is the microwave network analysis [14], and the other is simulating the diode grid by a linear equivalent circuit instead of a diode. In Section 4, the transmission property of the shield with respect to a broadband impulse is studied, where the diode is described by its SPICE circuit model including the nonlinear property. In Section 5, we study the UWB and impulse response of a diode grid valid for an arbitrarily polarized wave.

## 2. STRUCTURE AND PRINCIPLE OF THE SHIELD BASED ON A DIODE GRID

The structure of an electromagnetic shield based on a diode grid is shown in Figure 1(a). A thin planar diode grid is constructed from an infinite square mesh with space  $a = 10$  mm. Two diodes are anti-parallel arranged in the  $x$  direction in each unit cell. Thus the diode grid is only effective for the  $E$  component in the  $x$  direction. When an electromagnetic plane wave traveling in the  $z$  direction is perpendicularly incident upon the diode grid depicted in Figure 1(b), the electric field polarized in the  $x$  direction produces a voltage across the diode. When the input electromagnetic wave is weak, the diode is in “OFF” state. The vertical wire in the grid is open. The electromagnetic wave can go through the diode grid. When the input electromagnetic wave is strong, the diode is in “ON” state, the vertical wire is shorted and the electromagnetic wave is blocked by the diode grid.

The interaction of the wave with the diode grid was studied by a commercial EM simulation software integrated with the nonlinear SPICE circuit solver Wavenology<sup>TM</sup>. The simulation model of a unit cell is shown in Figure 1(c), where a periodic boundary condition setup in Wavenology<sup>TM</sup> was used to simulate a grid with an infinite number of diodes arranged periodically in the  $xy$  plane. The wire in the simulation is a perfect conductor with a cross-section of  $0.8 \times 0.8$  mm<sup>2</sup>. The diode used in EM simulation is an RF Schottky Barrier diode, which is described by a SPICE circuit model. The SPICE model provided by the manufacture is [15],

```
.model HMPS282 D (IS=22000p RS=8.0 BV=15 IBV=0.1 m
                  CJO=0.7p M=0.5 N=1.08).
```

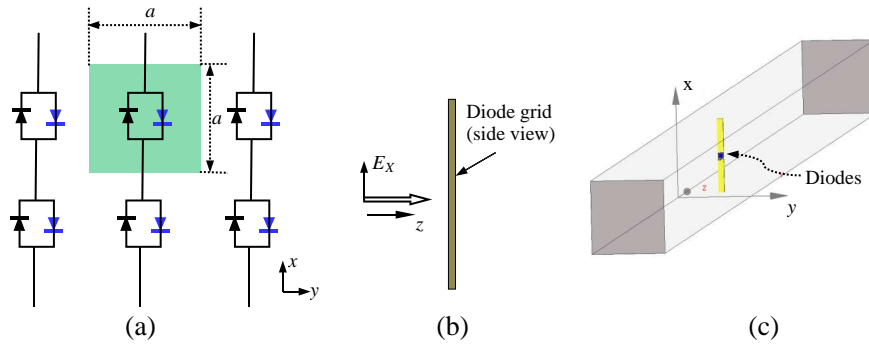


**Figure 1.** Wave incident upon an infinite diode grid and the simulation model. (a) Structure of a diode grid with the unit cell size as  $a = 10$  mm. Diodes are anti-parallel arranged in  $x$  direction on the  $xy$  plane. (b) Electromagnetic wave incident upon the diode grid. (c) Simulation model using Wavenology<sup>TM</sup> with periodic boundary conditions in the  $x$  and  $y$  directions.

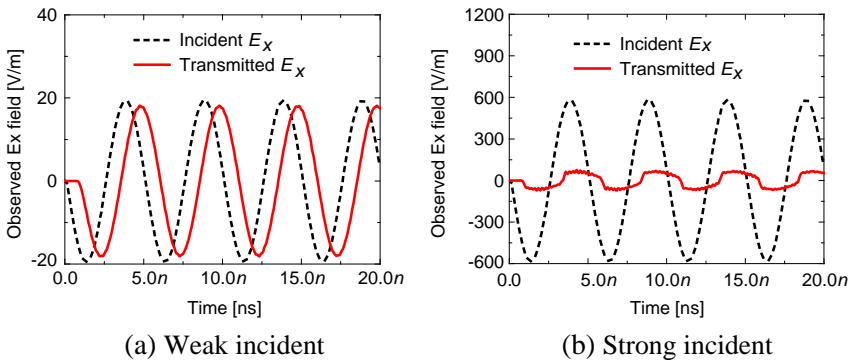


**Figure 2.** Simulated results of the incident and transmitted  $E_X$  field when a plane wave is perpendicularly incident upon a diode grid. (a) Weak incident with  $E_X = 19$  V/m. (b) Strong incident with  $E_X = 580$  V/m.

where  $IS$  is the saturation current;  $RS$  is the ohmic resistance;  $BV$  is the reverse breakdown;  $IBV$  is the current at  $BV$ ;  $CJO$  is the zero-bias junction capacitance;  $M$  is the junction capacitance grading exponent;  $N$  is the emission coefficient.

Figure 2 shows the simulated results of the incident and transmitted  $E_X$  field when a plane wave is perpendicularly incident upon a diode grid. The frequency of incident wave is 0.2 GHz, whose

wavelength  $\lambda$  is much larger than the grid space  $a$  ( $\lambda \gg a$ ). It is shown that a weak incident, for example  $E_X = 19$  v/m, can go through the diode grid. However, a strong incident wave, for example  $E_X = 580$  v/m, is blocked by the grid.

The simulation result confirms that the diode grid operates as a self-actuated PSS at the investigated frequency. The grid is frequency dependent because there are reactive elements in the diode grid, such as parasitic inductance from conducting wire and junction capacitance of the diode. In order to obtain a better knowledge on the performance of this shielding device, it is necessary to quantify the properties of a diode grid over a wide frequency band.

### 3. UWB RESPONSE OF A DIODE GRID IN THE FREQUENCY DOMAIN

The transmission and reflection coefficients at a single frequency can be calculated from the transmitted and reflected field with respect to the incident field. However, the coefficients over a wide frequency band cannot be correctly obtained by simulating the diode grid in the frequency domain because of the nonlinear property of a diode. To investigate the transmission and reflection properties of the diode grid over an ultra wide band, we use two linear analysis methods in this section. One method is the regular microwave network analysis [14]. Another is simulating the shield by a linear equivalent circuit instead of a diode.

As mentioned before, we use HMPS282 diode to build the grid. Figure 3(a) indicates the equivalent circuit for this diode.  $C_P$  and  $L_P$  are package capacitance and inductance, respectively.  $R_S$  accounts for contact and current-spreading resistance.  $R_J$  and  $C_J$  are the junction resistance and capacitance, respectively. Both of them are bias-dependent. Due to the small  $C_P$  and the small  $L_P$  are usually taken as 0 in the manufacturer datasheet, they are neglected in this paper. Figure 3(b) shows a transmission model for the unit cell of the diode grid, including the two anti-parallel diode arms. Each arm has a diode equivalent circuit in series with an inductive reactance  $L_W$  which is introduced by the grid wire.  $Z_0$  is the characteristic impedance of the transmission line. The model in Figure 3(b) is equal to the circuit shown in Figure 3(c), a free space transmission line shunted by a lumped admittance  $Y$ .

Using network analysis [14], we can calculate the transmission coefficient  $\tau$  and reflection coefficient  $\Gamma$  for the model in Figure 3(b)

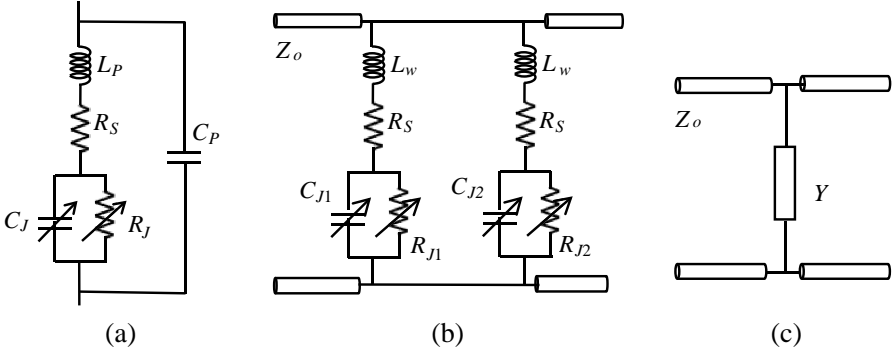


**Figure 3.** Diode grid analyzed by the microwave network model. (a) Equivalent circuit of diode. (b) Model for a unit cell in the anti-parallel diode grid. (c) Transmission model shunted with an admittance.

as,

$$\tau = \frac{2}{2 + Z_0 Y} \quad (1)$$

$$\Gamma = -\frac{Z_0 Y}{2 + Z_0 Y} \quad (2)$$

where  $Z_0$  is the characteristic impedance of free space, and  $Y = \frac{1}{Z_1} + \frac{1}{Z_2}$ ,

$$Z_1 = R_s + j\omega L_W + \frac{R_{j1}}{1 + jR_{j1}\omega C_{j1}}, \quad Z_2 = R_s + j\omega L_W + \frac{R_{j2}}{1 + jR_{j2}\omega C_{j2}}$$

. In the linear analysis in this section,  $R_S$ ,  $C_J$ ,  $R_J$  and  $L_W$  are set to fixed values to estimate the transmission and reflection properties of the diode grid.  $R_s$  is  $8.0\Omega$ , which is provided by the diode manufacture.  $C_J$  is set as the value of zero-bias junction capacitance  $0.7\text{ pF}$ . According to diode linear equivalent circuit and  $I$ - $V$  data sheet at  $25^\circ\text{C}$  provided by manufacturer, the values of  $R_J$  in forward and reverse bias are  $2.0\Omega$  and  $0.4\text{ M}\Omega$ , respectively,  $L_W$  is estimated from the simulated result of the model shown in Figure 4, where the diode is replaced by a capacitor,

$$L_W = \frac{1}{(2\pi)^2 f^2 \times C} \quad (3)$$

where  $f$  is the simulated resonant frequency, and  $C$  is capacitance value. For the wire in a unit cell of the diode grid with  $a = 10\text{ mm}$ , the parasitic inductance is  $3.04\text{ nH}$ .

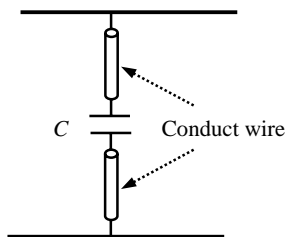


**Figure 4.** Simulation model to obtain  $L_W$  value in microwave network analysis of the diode grid.

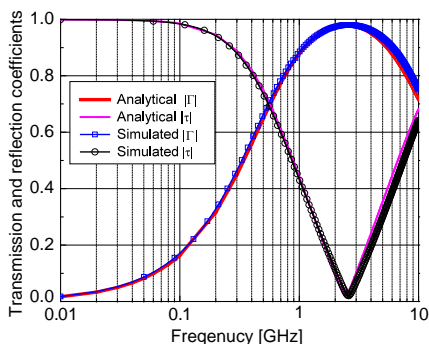


**Figure 5.** Transmission and reflection coefficients for the diode grid when the incident  $E$  field is weak.  $R_{J1} = R_{J2} = 0.4\text{ M}\Omega$ ,  $L_W = 3.04\text{ nH}$ ,  $C_J = 0.7\text{ pF}$ .

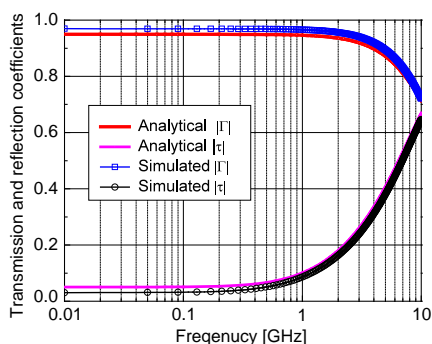


**Figure 6.** Transmission and reflection coefficients when the incident  $E$  field is strong.  $R_{J1} = 0.4\text{ M}\Omega$ ,  $R_{J2} = 2\text{ }\Omega$ ,  $L_W = 3.04\text{ nH}$ ,  $C_J = 0.7\text{ pF}$ .

Submitting these values for  $R_S$ ,  $C_J$ ,  $R_J$  and  $L_W$  to Eq. (1) and Eq. (2), the transmission coefficient  $\tau$  and reflection coefficient  $\Gamma$  are calculated respecting to the frequency of the incident electromagnetic field. The simulation in the frequency domain is also carried out to obtain the coefficients, where diode is replaced by using  $R_S$ ,  $C_J$  and  $R_J$ . Figure 5 shows the results when the incident  $E_X$  field is weak. In this case,  $R_J$  value for both diodes in a unit cell is  $0.4\text{ M}\Omega$ . The analytical solution from the network analysis agrees well with the simulated result. The diode grid is transparent for the weak signal with a low frequency. However, there is a stop band around  $2.3\text{ GHz}$ . If the frequency of incident signal is in the stop band, the signal will be blocked by the diode grid even it is weak.

The analytical and simulated results for a strong incident  $E$  field

are shown in Figure 6. In this case,  $R_{J1}$  value is  $0.4M\Omega$ , and  $R_{J2}$  value is  $2.0\Omega$ . It is shown that the diode grid can effectively prevent the transmission of the strong wave at a low frequency. However, the diode grid works not very well in the high frequencies. The transmission coefficient increases when the frequency becomes high. For a strong incident wave with frequency higher than 7.0 GHz, the transmission coefficient by the grid is larger than 0.5.

The results in Figure 5 and Figure 6 indicate that the diode grid is highly frequency dependent. This is contributed by the reactive components of the diode grid, the parasitic inductance  $L_W$  and the junction capacitance  $C_J$ . In order to clarify the effect from  $L_W$  and  $C_J$ , the calculated transmission coefficient for three kinds shield are compared in Figure 7. These three kinds of shield all have the diode arrangement as Figure 1(a). The diodes and the grid parameters are summarized in Table 1.

**Table 1.** Three kinds of shield for comparison.

	Diode	Unit cell size [mm]	$L_W$ [nH]	$C_J$ [pF]
Shield A	HMPS282	10	3.04	0.7
Shield B	DMK2308	10	3.04	0.05
Shield C	DMK2308	3	0.3	0.05

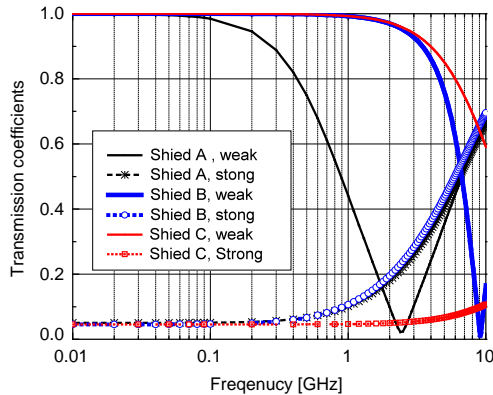


**Figure 7.** Calculated transmission coefficient for the Shield A, B and C. The results for weak and strong incident are shown.

As listed in Table 1, Shield A has large  $L_W$  and  $C_J$ . Shield B has the same unit cell (same  $L_W$  value) as Shield A. However, it is constructed by Schottky diode DMK2308, which has a small zero

junction capacitance [16]. Shield C has both smaller values of  $L_W$  and  $C_J$  compared to shield A. Figure 7 shows that, for a weak incident, a smaller  $L_W$  and  $C_J$  will shift the stop band to a higher frequency; for a strong incident, a very small transmission coefficient can be kept up to 10 GHz.

#### 4. BROADBAND IMPULSE RESPONSE OF A DIODE GRID IN THE TIME DOMAIN

UWB response in Section 3 shows that a diode grid can operate as self-actuated protection over a wide frequency range. The operating frequency band can be further extended wider by smaller  $L_W$  and  $C_J$ . UWB response of a diode grid indicates that the diode grid can be used to protect electronic components and systems from the intentional or unintentional broadband impulse electromagnetic interference (EMI). In this section, the transmission property of the diode grid is investigated with a broadband incident impulse. This is simulated by Wavenology<sup>TM</sup>, where the diode is described by a SPICE circuit model including the nonlinear property.

Figure 8 indicates the simulated results of an incident wave and the transmitted wave through Shield A. The incident wave has a form of 1st order Black-Harris Window (BHW1) function. The frequency range of the incident wave is  $[f_L, 100 * f_L]$ , where  $f_L = 0.01$  GHz for Figure 8. The result in Figure 8(a) shows that a weak incident impulse can go through Shield A. Figure 8(b) indicates that a strong impulse is significantly suppressed by the diode grid.

It is obvious that the protection effect by the diode grid depends on the frequency range of the impulse. Figure 9 shows the simulated results when the incident wave has a frequency range of 0.1–10.0 GHz, which is higher than that for Figure 8. Figure 9(a) shows the penetrating  $E_x$  for shield A, B and C when the incident wave is weak. Shield A blocks an impulse having a frequency range of 0.1–10.0 GHz. This is contrast to that it is almost transparent for a BHW1 impulse of 0.01–1.0 GHz as shown in Figure 8(a). Shield C permits a BHW1 impulse of 0.1–10.0 GHz to be transparent because it has small transmission in this frequency band. Figure 9(b) is the result when the incident wave is strong. The wave is blocked by all three kinds of shield because there is no pass band in this frequency range.

The simulated results show that a diode grid can prevent a broadband impulse EMI. Due to the fact that a diode grid is highly frequency dependent, a shield for a broadband impulse with high frequency components should choose small  $L_W$  and small  $C_J$ .

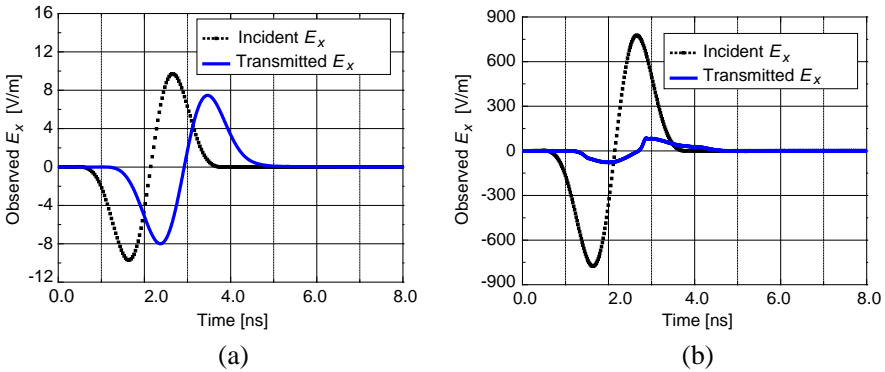


**Figure 8.** Simulated results of the incident and transmitted  $E_X$  field through Shield A. The incident wave is described by a BHW1 function with frequency range of [0.01, 1.0] GHz. (a) Weak incident field. (b) Strong incident field.

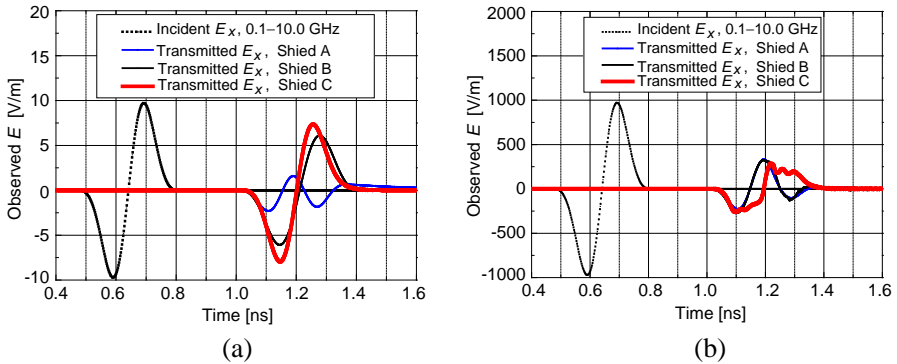


**Figure 9.** Simulated results of the incident and transmitted  $E_X$  field through Shield A, B and C. The incident wave is described by a BHW1 function with frequency range of [0.1, 10.0] GHz. (a) Weak incident field. (b) Strong incident field.

## 5. UWB (FREQUENCY) AND IMPULSE (TRANSIENT) RESPONSES OF AN ORTHOGONAL DIODE GRID

The diode grid shown in Figure 1(a) is an effective self-actuated PSS for an incident  $E$  field polarized in  $x$  direction. To protect the system from an arbitrarily polarized wave, an orthogonal diode grid as shown in Figure 10(a) can be used. In this section, we study UWB and impulse properties of this grid by Wavenology<sup>TM</sup>. Figure 10(b) depicts

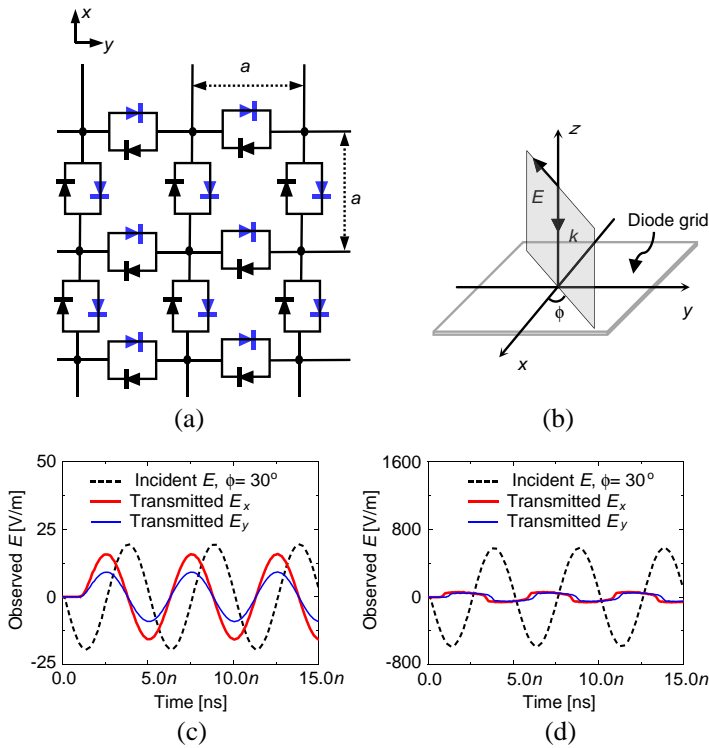


**Figure 10.** A plane wave incident upon an orthogonal diode grid. (a) Structure of the orthogonal diode grid. (b) A plane wave perpendicularly incident upon the diode grid.  $E$  polarization is in a direction of  $\phi = 30^\circ$ . (c)  $E$  fields in simulations when the incident wave is weak  $E = 19$  V/m. (d)  $E$  fields in simulation when the incident wave is strong  $E = 580$  V/m.

that an electromagnetic wave is incident upon the orthogonal diode grid with a  $E$  polarization  $\phi = 30^\circ$ . When the incident is weak, the diodes in  $x$  and  $y$  directions both are in OFF state. The field components in  $x$  and  $y$  directions go through the diode grid, as shown in Figure 10(c). When the incident is strong, the diodes are in ON state and the fields components in  $x$  and  $y$  directions are blocked, as indicated in Figure 10(d).

Additional to the property at a single frequency, Figure 11 and Figure 12 indicate UWB and impulse response of the orthogonal diode grid, respectively. Figure 11 shows the transmission coefficient of the orthogonal diode grid over 0.01–10.0 GHz frequency range when the  $E$

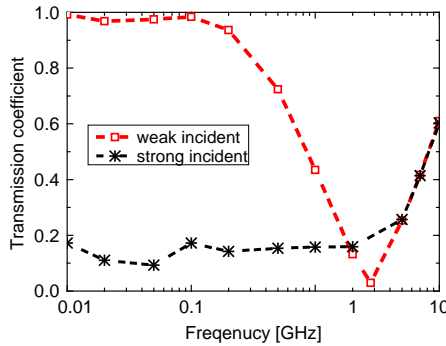


**Figure 11.** Transmission coefficients over 0.01–10.0 GHz frequency range for the orthogonal diode grid when the  $E$  field polarization of the incident wave is in the direction of  $\phi = 30^\circ$ .

polarization of the incident wave is in the direction of  $\phi = 30^\circ$ . The transmission coefficient is obtained by the transient simulation with frequency sweeping. Strong frequency dependence by the orthogonal diode grid can be observed, especially for a weak incident wave. Figure 12 shows the simulated results of the incident  $E$  field and  $E$  field behind the orthogonal diode grid. The incident field for simulation is a broadband signal described as a 0.01–1.0 GHz BHW1 function. The  $E$  field polarization is in the direction of  $\phi = 30^\circ$ . Figure 12(a) shows that a weak incident impulse can go through the diode grid. Figure 12(b) indicates that the transmitted signal is much smaller than the incident signal when the incident impulse is strong.

The results in Figure 11 and Figure 12 are obtained assuming that the  $E$  field polarization is in the direction of  $\phi = 30^\circ$ . Figure 13 shows the simulated results of transmission coefficient  $\tau$  when  $\phi$  changes from 0 to  $90^\circ$  for both weak and strong incident. The values of  $\tau$  keep almost same when  $\phi$  changes. Consequently, an orthogonal diode grid is a good shield for the  $E$  field in an arbitrary polarization.

It can be seen that the transmission property of the investigated orthogonal diode grid is similar to that of the diode grid shown in Figure 1(a), i.e., Shield A, which is effective for  $x$  polarization wave. It is also clarified that the transmission property of an orthogonal diode grid is almost independent of the incidence angle  $\phi$ . These are based on the fact that the  $x$  and  $y$  components of an incident wave are filtered by the same anti-parallel diodes spaced in the same distance  $a = 10$  mm. The results show that we can estimate the property of an orthogonal diode for arbitrary polarization direction by studying a diode grid only valid for an incident wave at a specific direction.

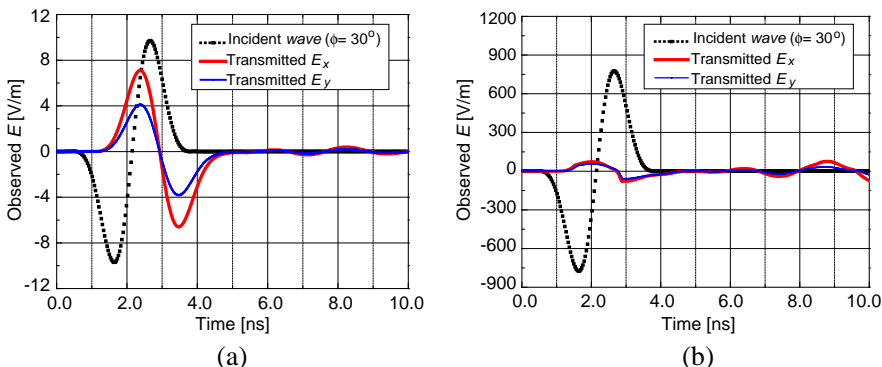


**Figure 12.** Simulated results for the incident  $E$  field and the  $E$  field behind the orthogonal diode grid when the incident field is an impulse described as a 0.01–1.0 GHz BHW1 function. The  $E$  field polarization is in the direction of  $\phi = 30^\circ$ . (a) Weak incident field. (b) Strong incident field.

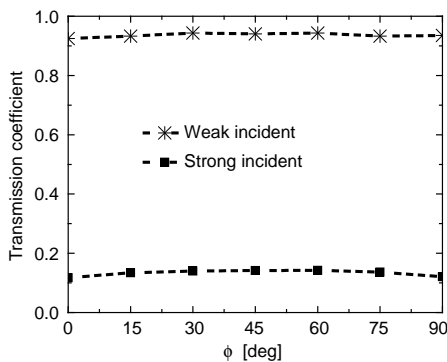


**Figure 13.** The simulated results of the transmission coefficient  $\tau$  when  $\phi$  changes for  $0^\circ$  to  $90^\circ$  for both weak and strong incident.

## 6. CONCLUSION

This paper investigates the UWB and impulse response of an electromagnetic wave shield based on a diode grid by the network analysis and by a commercial full wave transient field simulator integrated with the nonlinear SPICE circuit solver. In the frequency domain, the reflection and transmission properties of the diode grid are studied over the frequency range from 0.01 to 10 GHz. In the investigated low frequency range, the diode grid operates as a self-

actuated electromagnetic PSS. At high frequency range, the diode grid does not work very well because of the reactive elements in the diode grid. To extend the operating frequency of the diode grid to high band, it is necessary to reduce unit cell size, and choose the diode with small junction capacitance. In the time domain, the transmission property of the shield is studied with respect to a broadband signal, which has a form of BHW1 function in the frequency range of  $[f_L, 100 * f_L]$ . The result shows that the diode grid can protect electronic components and systems from broadband impulse EMI. Similar to the UWB response, the frequency range of impulse to be protected by the diode grid depends on the unit cell size of diode grid and the junction capacitance of diode. The paper also investigates the UWB and impulse response for an orthogonal diode grid. The relationship between the transmission coefficient  $\tau$  and the incident  $E$  field polarization angle  $\phi$  is obtained. The results show that the orthogonal diode grid is effective for an arbitrarily polarized incidence wave.

## ACKNOWLEDGMENT

The authors sincerely thank Wave Computation Technologies Inc. for providing Wavenology EM, a 3D joint electromagnetic wave and circuit simulation software, and for their generous technical support during the study process.

## REFERENCES

1. Ulrich, R., "Far-infrared properties of metallic mesh and its complementary structure," *Infrared Physics*, Vol. 7, 37–55, 1967.
2. Christodoulou, C. and J. Kauffman, "On the electromagnetic scattering from infinite rectangular grids with finite conductivity," *IEEE Transactions on Antennas and Propagation*, Vol. 34, No. 2, 144–154, 1986.
3. Kikel, A., L. Altgibers, and I. Merritt, "Plasma limiters," AIAA Paper, AIAA-98-2564, 1998.
4. Mankowski, J. J., D. Hemmert, A. Neuber, and H. Krompholz, "Field enhanced microwave breakdown in a plasma limiter," *IEEE Trans. Plasma Sci.*, Vol. 30, No. 1, 102–103, 2002.
5. Yang, G., J. C. Tan, D. Y. Sheng, and Y. C. Yang, "Plasma limiter for protecting against high power microwave," *J. Sci. Ind. Res.*, Vol. 67, 685–687, 2008.

6. Altgilbers, L., S. Balevicius, O. Kiprijanovic, V. Pyragas, E. E. Tornau, A. Jukna, B. Vengalis, and F. Anisimovas, "Fast protector against EMP using electrical field induced resistance change in La Ca MnO thin films," *Proc. IEEE Int. Conf. Pulsed Power Plasma Sci.*, Vol. 2, 1782–1785, 2001.
7. Barthelemy, A., A. Fert, J. P. Contour, M. Bowen, V. Cros, J. M. DeTeresa, A. Hamzic, J. C. Faini, J. George, J. Grollier, F. Montaigne, F. Pailloux, F. Petroff, and C. Voillaume, "Magnetoresistance and spinelectronics," *J. Magn. Magn. Mater.*, Vols. 242–245, 68–76, 2002.
8. Chang, T. K., R. J. Langley, and E. Parker, "An active square loop frequency selective surface," *IEEE Microwave Guided Wave Lett.*, Vol. 3, No. 10, 387–388, 1993.
9. Sanz-Izquierdo, B., E. A. Parker, J. B. Robertson, and J. C. Batchelor, "Tuning technique for active FSS arrays," *Electronics Letters*, Vol. 45, No. 22, 1107–1109, 2009.
10. Kiani, G. I., K. L. Ford, L. G. Olsson, K. P. Esselle, and C. J. Panagamuwa, "Switchable frequency selective surface for reconfigurable electromagnetic architecture of buildings," *IEEE Transactions on Antennas and Propagation*, Vol. 58, No. 2, 581–584, 2010.
11. Monni, S., D. J. Bekers, M. van Wanum, R. van Dijk, A. Neto, G. Gerini, and F. E. van Vliet, "Limiting frequency selective surfaces," *Proc. 2009 European Microwave Conference (EuMC)*, 606–609, 2009.
12. Yang, C., P. G. Liu, and X. J. Huang, "A novel method of energy selective surface for adaptive HPM/EMP protection," *IEEE Antennas and Wireless Propagation Letters*, Vol. 12, 112–115, 2013.
13. <http://www.wavenology.com/>.
14. Pozar, D. M., *Microwave Engineering*, 3rd Edition, John Wiley & Sons, Inc., 2009.
15. HMPS-282x series Datasheet, <http://www.avagotech.com/>.
16. DMK2308 series Datasheet, <http://www.skyworksinc.com>.